

Manuscript Draft: Aim3 Leaf Traits

Bolívar Aponte Rolón Mareli Sánchez Juliá
A. Elizabeth Arnold Sunshine A. Van Bael

2023-12-06

1 Abstract

2 Introduction

3 Methods

3.1 Field

Growth and host plant inoculation seven tropical tree species was conducted at the greenhouses in the Gamboa Research Station, Smithsonian Tropical Research institute, Republic of Panama. The species, *Theobroma cacao*, *Dypterix* sp., *Lacmellea panamensis*, *Apeiba membranacea*, *Heisteria concinna*, *Chrysophyllum caimito*, and *Cordia alliodora* were chosen due to their variance in leaf traits (J.Wright unpublished data) and the availability of seeds in January- April 2019. Seeds of tree species were collected from the forest floor and grown in the greenhouse. Seedlings were kept in a chamber made out of PVC and clear plastic

to prevent inoculation from spore fall inside the greenhouse. NEEDS INFORMATION ON THE SOIL MIXTURE AND AUTOCLAVING PROTOCOL. Seedlings reached a minimum of 4 true leaves before endophyte inoculation. Then 10 individual plants of each species were exposed to 10 nights of spore fall to achieve a high endophyte load (E+) and 10 homologous plants were kept inside the greenhouse plastic chamber to maintain a low endophyte load (E-) (Fig. ? MAKE A DIRAGRAM?). Plants exposed to spore fall were placed near (~10 m) the forest edge at dusk (~18:00 hours) and returned to the greenhouse at dawn (~07:00 hours) (Bittleston et al. 2011).

3.1.1 Leaf trait measurements

Three mature leaves were haphazardly collected from each of the individual plants in each treatment (E+, E-) within 7-10 days after inoculation treatment. Anthocyanin (ACI) content and leaf thickness (LT) were measured while the leaf was still attached to the plant. We measured anthocyanin content with ACM-200plus (Opti-Sciences Inc. Hudson, New Hampshire, U.S.A.) on three haphazardly selected locations (working from the petiole out to the leaf tip) on the leaf surface of three haphazardly selected leaves for a total of nine measurements per plant (Tellez et al., 2022). The ACM-200 calculates an anthocyanin content index (ACI) value from the ratio of % transmittance at 931 nm/% transmittance at 525 nm (**opti-sciencesinc?**) . On compound leaves (i.e., *Dypterix* sp.) we measured at three different leaflets. Leaf thickness (m) was measured with a Mitutoyo 7327 Micrometer Gauge (Mitutoyo, Takatsu-ku, Kawasaki, Japan) in sthe same manner as the anthocyanin measurements, taking care to avoid major and

secondary veins. After anthocyanin and leaf thickness measurements were completed, we re-moved the leaves from their stems, placed them inside a plastic bag (i.e. Ziploc), place in an ice chest and moved them to the lab for further measurements. Leaf punch strength (LPS) was measured with an Imada DST-11a digital force gauge (Imada Inc., Northbrook, IL, United States) by conducting punch-and-die tests with a sharp-edged cylindrical steel punch (2.0 mm diameter) and a steel die with a sharp-edged aperture of small clearance (0.05 mm). The leaf punch measurements were taken by puncturing the leaf lamina at the base, mid-leaf and tip on both sides of the mid-vein, avoiding minor leaf veins when possible (Tellez et al., 2022). Once leaf toughness was measured, we used a 7 mm diameter punch hole to puncture disks for leaf mass per area (LMA) measurements. We collected one three disks per leaf (see Supplementary material for details). The disk punches dried at 60 °C for 48-72 hours. before being weighed.

3.1.2 Leaf tissue preparation for molecular work

The selected leaves were also used to profile endophyte community composition, abundance, and richness via amplicon sequencing (Illumina MiSeq). The leaf tissue remaining after the leaf trait measurements had the main vein and margins excised so that only the lamina remained. The lamina was haphazardly cut into 2 x 2 mm segments, enough to obtain a total of 16, and surface sterilized by sequential rinsing in 95% ethanol (10 s), 0.5 NaOCl (2 mins) and 70% ethanol (2 mins), as per (Arnold et al., 2003; Higgins et al., 2014; Tellez et al., 2022). After, leaves were air-dried briefly under sterile conditions. Sixteen leaf segments per leaf, a total of forty-eight leaf segments per plant, were plated in 2% malt extract agar (MEA), sealed with

56 Parafilm M (Bemis Company Inc., U.S.A.) and incubated at room temperature. The cultured
57 leaf segments were used to estimate endophyte colonization of E+ and E- leaves. The presence
58 or absence of endophytic fungi in the leaf cuttings was assessed 7 days after plating. The
59 remaining sterilized leaf lamina was preserved in sterile 15 mL tubes with ~ 10 mL CTAB
60 solution (1 M Tris-HCl pH 8, 5 M NaCl, 0.5 M EDTA, and 20 g CTAB). Leaf tissue in CTAB
61 solution was used for amplicon sequencing (described in detail below). All leaf tissue handling
62 was performed in a biosafety cabinet with all surfaces sterilized by exposure to UV light for
63 30 minutes and cleaned sequentially in between samples with 95% ethanol, 0.5% NaOCl and
64 70% ethanol to prevent cross contamination.

65 **3.2 Amplicon sequencing**

66 Leaf tissue in CTAB solution was stored for 2 months at room temperature prior to being
67 placed at -80 C for 3 months before extracting DNA. In preparation for DNA extraction, we
68 decontaminated all instruments, materials, and surfaces with DNAway (Molecular BioProducts
69 Inc., San Diego, CA, United States), 95% Ethanol, 0.5 % NaOCl, and 70 % Ethanol, and
70 subsequently treated with UV light for 30 minutes in biosafety cabinet. We then transferred 0.2
71 – 0.3 g of leaf tissue into duplicate sterile 2mL tubes, resulting in 2 subsamples. Total genomic
72 DNA from subsamples was extracted as described in U'Ren & Arnold (2017). In brief, we added
73 two sterile 3.2 mm stainless steel beads to each tube and proceeded to lyophilize samples for 72
74 hours to fully remove CTAB content from tissue. After this period, we submerged the sample
75 tubes in liquid nitrogen for 30s and proceeded to homogenize samples to a fine powder for 45 s

76 in FastPrep-24 Tissue and Cell Homogenizer (MP Biomedicals, Solon, OH, USA). Afterwards,
 77 we repeated the decontamination procedure described before and used QIAGEN DNeasy 96
 78 PowerPlant Pro-HTP Kit (U'Ren & Arnold, 2017) (QIAGEN, Valencia, CA, USA). After all
 79 genomic DNA was extracted, we pooled the subsamples for each individual sample before
 80 amplification. We used sterile equipment and pipettes with aerosol-resistant tips with filters
 81 in all steps before amplification. We followed a two-step amplification approach previously
 82 described by Sarmiento et al. (2017) and U'Ren & Arnold (2017). We used primers for
 83 the fungal ITSrDNA region, ITS1f (5'-CTTGGTCATTTAGAGGAAGTAA-3') and ITS4 (5'-
 84 TCCTCCGCTTATTGATATGC-3') with modified universal consensus sequences CS1 and CS2
 85 and 0–5 bp for phase-shifting. Every sample was amplified in two parallel reactions containing
 86 1–2 µL of DNA template (U'Ren & Arnold, 2017; see also Tellez et al., 2022). We visualized
 87 PCR (PCR1) reactions with SYBR Green 1 (Invitrogen, Carlsbad, CA, USA) on 2% agarose
 88 gel (Oita et al., 2021). Based on the electrophoresis band intensity, we combined parallel PCR1
 89 reactions and diluted 5 µL of amplicon product with molecular grade water to standardize to
 90 a concentration of 1:15 (Sarmiento et al., 2017 for details; Tellez et al., 2022). We included
 91 DNA extraction blanks and PCR1 negatives in this step. We used a separate set of sterile
 92 pipettes, tips, and equipment to reduce contamination. We used a designated PCR area to
 93 restrict contact with pre-PCR materials (Oita et al., 2021).
 94 We used 1 µL of PCR1 product from samples and negative control for a second PCR (PCR2)
 95 with barcode adapters (IBEST Genomics Resource Core, Moscow, ID, USA). Each PCR2
 96 reaction (total 15 µL) contained 1X Phusion Flash High Fidelity PCR Master Mix, 0.075 µM

97 of barcoded primers (forward and reverse pooled at a concentration of 2 μ M) and 0.24mg/mL
98 of BSA following Sarmiento (2017) and U'Ren & Arnold (2017). Before final pooling for
99 sequencing, we purified the amplicons using Agencourt AMPure XP Beads (Beckman Coulter
100 Inc, Brea, CA USA) to a ratio of 1:1 following the manufacturer's instructions. The products
101 were evaluated with Bio Analyzer 2100 (Agilent Technologies, Santa Clara, CA, USA) (Tellez
102 et al., 2022). We quantified the samples through University of Arizona Genetics Core, and
103 subsequently diluted them to the same concentration to prevent over representation of samples
104 with higher concentration, see (CITATION). Amplicons were normalized to 1 ng/ μ L, then
105 pooled 2 μ L of each for sequencing. No contamination was detected visually or by fluorometric
106 analysis. To provide robust controls we combined 5 μ L of each PCR1 negative and the DNA
107 extraction blanks and sequenced them as samples. Ultimately, we combined samples into
108 a single tube with 20 ng/ μ L of amplified DNA with barcoded adapters for sequencing on
109 the Illumina MiSeq platform with Reagent Kit v3 (2×300 bp) following protocols from the
110 IBEST Genomics Resource Core at the University of Idaho, USA. Again, we included the DNA
111 extraction blanks and two PCR1 negatives and sequenced with samples. Sequencing yielded
112 3,778,081 total ITS1 reads.

113 **3.2.1 Mock Communities**

114 We processed and sequenced 12 mock communities following the methods described above.
115 This allowed us to assess the quality of our NGS data set. We used two mock communities
116 that consisted of PCR product from DNA extractions of 32 phylogenetically distinct fungi,

117 representing lineages that are typically observed as endophytes: Ascomycota, Basidiomycota,
118 Zygomycota and Chytridiomycota (Oita et al., 2021; see Daru et al., 2019 for details). In
119 brief, we used six mock communities with equimolar concentrations of DNA from all 32 fungal
120 taxa and another six mock communities with tiered concentrations of DNA from the same
121 fungal taxa (Daru et al., 2019). Each mock community was sequenced five times (i.e., five
122 replicates) (Oita et al., 2021). The read abundance from the equimolar and tiered communities
123 was positively associated with the expected read number (with replicates as a random factor:
124 $R^2_{Adj} = 0.87$, $P = XXXX$, see Supplementary Material). Using mock communities allowed us
125 to evaluate the sequencing effectiveness in communities with known composition and structure
126 (Bowman & Arnold, 2021). Henceforth, we used read abundance as a relevant proxy for
127 biological OTU abundance (U'Ren et al., 2019).

128 **3.2.2 Bioinformatic analyses**

129 We used VSEARCH (v2.14.1) for *de novo* chimera detection, dereplication and sequence align-
130 ment. VSEARCH is an open-source alternative to USEARCH that uses an optimal global
131 aligner (full dynamic programming Needleman-Wunsch), resulting in more accurate alignments
132 and sensitivity (Rognes et al., 2016). For mock communities and experimental samples, we
133 used forward reads (ITS1) for downstream bioinformatics analyses due to their high quality,
134 rather than reverse reads (ITS4). Following Sarmiento et al. (2017), we concatenated all reads
135 in a single file and used FastQC reports to assess Phred scores above 30 and determine the ad-
136 equate length of truncation. We processed 892,713 of sequence reads from mock communities

137 and 3,778,081 from experimental samples. We truncated mock community and experimental
138 sample reads to a length of 250 bp with command `fast_trunclen` and filtered them at a max-
139 imum expected error of 1.0 with command `fast_maxee`. We then clustered unique sequence
140 zero radius OTUs (that is, zOTUs; analogous to amplicon sequence variants (Callahan et al.,
141 2016)), by using commands `derep_fulllength` and `minseqlength` set at 2. Sequentially we
142 denoised and removed chimeras from read sequences with commands `cluster_unoise`, and
143 `uchime3_denovo`, respectively (see Supplementary YYY for details). Finally, we clustered
144 zOTUs at a 95% sequence similarity with command `usearch_global` and option `id` set at
145 0.95. After which, 3,035,960 sequence reads from experimental samples remained.

146 Taxonomy was assigned with the Tree-Based Alignment Selector Toolkit [v2.2; Carbone et
147 al. (2019)] by placing unknowns within the Pezizomycotina v2 reference tree (Carbone et al.,
148 2017). ITS sequences were blasted against the UNITE database by the ribosomal database
149 project (RDP) classifier. A total of 2147 OTUs hits were obtained and are composed of
150 68.6% Ascomycota, 26.8% Basidiomycota, <0.05% Chytridiomycota, <0.05% Glomeromycota,
151 <0.05% Mortierellomycota, <0.05% Rozellomycota, 0.05% Kickxellomycota, and 4.2 % BLAST
152 hit misses. Only OTUs representing Ascomycota were used for downstream statistical analyses
153 since foliar endophyte communities in tropical trees are dominated by Ascomycota (Arnold &
154 Lutzoni, 2007).

155 For each OTU identified, we removed laboratory contaminants from experimental samples by
156 subtracting the average read count found in control samples from the DNA extraction and
157 PCR steps. Our analysis of mock communities allowed use to identify and remove false OTUs

from experimental samples, those with fewer than 10 reads, and remove 0.1% of the read relative abundance across all samples (Oita et al., 2021). Removed reads represent the frequency of reads classified as contamination in the mock communities relative to the expected read count. Three experimental samples from *Theobroma cacao* ($n=2$) and *Apeiba membranacea* ($n=1$) were removed from all analyses due to incomplete entries. After pruning taxa with zero reads from experimental samples, we identified 260 OTUs found exclusively in control ($E-$) plants ($n=78$) and deemed them as artifacts resulting from the greenhouse conditions. Consequently, these were consistently eliminated from treatment ($E+$) plants across all species. We converted reads for each fungal OTU to proportions of total sequence abundance per sample to reduce differences in sampling effort, following previous studies (Weiss et al. (2017); McMurdie & Holmes (2014)). We then removed singletons and obtained an average of 2,464,558 sequence reads in 529 Ascomycota OTUs across 156 experimental samples of 7 tree species. All analyses post taxonomic assignment were performed in R [v. 4.3.2; R Core Team (2023)] using the **phyloseq** package (McMurdie & Holmes, 2013) and custom scripts (see Supplementary Material).

3.2.3 Ant-endophyte interaction assays

A fresh fourth leaf was used in ant assays. To assess leaf-cutter ant damage, we introduced one detached leaf per plant per treatment to an actively foraging leaf-cutter ant colony for a two-hour assay. We presented leaf-cutter ant colonies with a choice of an $E+$ or an $E-$ leaf on one disposable plastic plate next to an active nest trail. Carefully, we collected and placed

178 debris from the trail leading up to the plate to lure ants into the plate. We initiated the ant
179 assay as soon as one ant entered the plate and explored the leaf contents (for ~ 10-20 seconds).
180 Every five minutes we took a digital photo of the choice arena until about 75% of the leaf
181 content of one of the leaves was consumed. We used the digital photo at time zero and at the
182 end of trial to quantify the leaf area removed using ImageJ [v1.52r; Schneider et al. (2012)].
183 Ant recruitment was estimated by counting individuals in the choice arena throughout trial
184 event.

185 **3.2.4 Pathogen assays**

186 For the pathogen assays, we introduced an agar plug inoculated with hyphae of *Calonectria* sp.
187 ($P+$ treatment), and an agar plug without the pathogen ($P-$ control) to similarly aged/sized
188 leaves within 10-14 days after endophyte inoculations (CITATION). Leaves with the $P+$ or
189 $P-$ treatment were misted with sterile water two times a day (morning and afternoon) to
190 maintain moisture. After four days, we removed the plugs and took digital photos to analyze
191 leaf area damage using ImageJ [v1.52r; Schneider et al. (2012)].

192 **3.2.5 Statistical Analyses**

193 We explored how leaf functional traits and foliar fungal symbionts correlated to herbivory and
194 pathogen damage on leaves. We present the analyses at the leaf and at the plant level. Leaf
195 functional traits were measured and are presented in their raw form, at the leaf level, while

FEF data was explored and is presented at the plant level. In analyses where leaf functional traits and FEF are combined we used averages of the leaf functional traits.

To test for H2, we used a general linear mixed model (GLM) with XXXX as the response variable. To determine which fixed effects to include in the models we used the `vif` function in *R* to calculate the variance inflation factor for all explanatory variables (ACI, LT, LPS and LMA) (R Core Team, 2023). We then created a correlation matrix with `cor` function to assess correlations among covariates. We opted to maintain explanatory variables pertaining to physical barriers (LT, LPS and LMA) and exclude ACI from subsequent linear models due to high collinearity with LPS (0.54) and LMA (0.73). Every variable kept exhibits some degree of collinearity and this is well recorded in the literature (CITE HERE).

Additionally, Principal Component Analysis (PCA) was used to reduce dimensions among covariates and reveal underlying interactions that could influence fungal endophyte abundance, diversity and community composition in seedlings. The PCA was computed using the `prcomp` function in *R* statistical software (R Core Team, 2023). A complete PCA was computed with variables ACI, LT, LPS, and LMA (FIGURE 2a?). We then proceeded to compute a PCA with the data from leaves of plants used in the ant ($n = 210$) and pathogen assays ($n = 192$).

The PCA revealed how covariates (LMA, ACI, Thickness and Toughness) interact. I overlapped tree species groups on the PCA axes to show how the variance in the data is explained by PC1 (60%) and PC2 (27%) (Fig. 4). This is indicative of correlation among covariates. Thickness and toughness were orthogonal to each other in PCA, indicative of low correlation.

216 4 Figures

217 [1] 1219

218 [1] 959

219 phyloseq-class experiment-level object

220 otu_table() OTU Table: [260 taxa and 78 samples]

221 sample_data() Sample Data: [78 samples by 8 sample variables]

222 tax_table() Taxonomy Table: [260 taxa by 7 taxonomic ranks]

223 Observed Shannon

224 APE10 14 2.51520076

225 APE20 31 2.70075742

226 APE21 57 3.19076122

227 APE23 52 3.06446621

228 APE24 15 1.23478277

229 APE25 57 3.40428531

230 APE26 22 2.63977664

231 APE27 40 2.84786599

232 APE29 54 3.19704154

233 APE02 21 1.79838935

234 APE03 11 1.81425152

235	APE04	44	3.22165864
236	APE05	28	2.27862971
237	APE06	23	1.26631613
238	APE08	19	1.62169096
239	APE09	17	2.49031735
240	DYP10	75	3.00927444
241	DYP11	34	2.61594706
242	DYP12	29	1.86504639
243	DYP13	46	2.17204233
244	DYP14	64	3.54471539
245	DYP15	23	2.11203370
246	DYP16	23	1.68619762
247	DYP17	44	2.91318626
248	DYP18	52	3.36226609
249	DYP01	49	3.15963210
250	DYP20	31	2.48571444
251	DYP21	53	1.89357794
252	DYP22	36	2.33230570
253	DYP23	42	1.07068302
254	DYP24	31	2.10404188
255	DYP25	85	3.58682413
256	DYP26	36	2.72051711

257	DYP27	65	3.27788974
258	DYP28	17	2.17219809
259	DYP29	46	1.95516756
260	DYP02	78	3.58101251
261	DYP31	14	0.49008950
262	DYP32	41	2.90159635
263	DYP33	52	3.15514489
264	DYP34	29	1.75216192
265	DYP03	38	2.40969901
266	DYP04	67	3.71729443
267	DYP05	28	1.32316928
268	DYP06	44	1.22022697
269	DYP07	47	1.61788738
270	DYP08	55	2.28334725
271	DYP09	45	1.49019056
272	HEI01	33	2.37010618
273	HEI02	54	3.17779272
274	HEI03	29	2.68466112
275	HEI04	63	3.34048945
276	LAC10	10	1.57151533
277	LAC11	5	0.16519758
278	LAC12	48	2.83431512

279	LAC01	20	1.40928003
280	LAC20	20	2.31186335
281	LAC21	41	2.97627565
282	LAC22	18	1.47489727
283	LAC23	51	3.23210677
284	LAC24	13	1.81906756
285	LAC25	24	2.25924579
286	LAC26	22	2.45947115
287	LAC27	51	3.24244149
288	LAC28	14	2.25781785
289	LAC29	31	2.94324769
290	LAC02	27	2.76884274
291	LAC03	56	2.04882240
292	LAC04	33	1.41319955
293	LAC05	28	2.03925482
294	LAC06	64	3.56409003
295	LAC07	17	1.77443643
296	LAC08	43	3.20470728
297	LAC09	49	2.42355752
298	THE010	32	1.53916205
299	THE001	22	1.67470563
300	THE020	12	1.25257407

301	THE021	45	2.12953170
302	THE022	21	1.10679641
303	THE023	38	1.33688253
304	THE025	19	0.87336680
305	THE026	17	1.98363582
306	THE027	18	1.11333111
307	THE028	33	1.84895676
308	THE029	18	1.13365210
309	THE002	55	2.79958184
310	THE004	38	2.48004419
311	THE005	31	2.45104841
312	THE006	39	2.21896015
313	THE007	18	0.97249801
314	THE008	22	1.58600019
315	APE01	15	0.84503373
316	APE22	14	2.02093030
317	APE28	15	1.82158050
318	APE07	16	2.30876804
319	COR10	107	3.84521918
320	COR01	13	0.74287401
321	COR20	31	3.03879253
322	COR21	94	3.70589228

323	COR22	36	3.24378024
324	COR23	76	3.22704436
325	COR24	60	3.28203843
326	COR25	66	3.37430673
327	COR26	17	2.22334542
328	COR27	103	3.44871403
329	COR28	21	2.25613532
330	COR29	5	1.60943791
331	COR02	86	3.45728943
332	COR03	23	2.48817714
333	COR04	96	3.81518747
334	COR05	22	2.51506724
335	COR06	2	0.43535370
336	COR07	36	2.82448004
337	COR08	91	3.78661499
338	COR09	68	3.33164374
339	CHRY10	52	3.10790600
340	CHRY11	14	2.63905733
341	CHRY12	47	2.77442801
342	CHRY01	13	2.56494936
343	CHRY20	43	2.90298300
344	CHRY21	67	2.96229747

345	CHRY22	45	2.89229670
346	CHRY23	55	2.90584215
347	CHRY24	49	2.83553024
348	CHRY25	34	1.54416540
349	CHRY26	30	2.85363827
350	CHRY27	23	0.90616341
351	CHRY28	12	2.06587056
352	CHRY29	6	1.67698777
353	CHRY02	16	2.71445235
354	CHRY03	20	2.84667964
355	CHRY04	48	3.25884573
356	CHRY05	39	2.93141239
357	CHRY06	62	2.32357172
358	CHRY07	24	2.51547623
359	CHRY08	11	2.36938212
360	CHRY09	23	2.00008850
361	HEI10	40	3.18527331
362	HEI20	13	1.74883522
363	HEI21	67	3.56258643
364	HEI22	36	1.52228148
365	HEI23	26	1.88207227
366	HEI24	26	2.55424287

367	HEI25	59	3.54251806
368	HEI26	35	2.79825779
369	HEI27	52	2.33842492
370	HEI28	12	0.37856063
371	HEI29	6	0.05397563
372	HEI05	37	2.50114755
373	HEI06	54	3.65566782
374	HEI07	12	1.20945765
375	HEI08	33	1.66551947
376	HEI09	17	1.91911330
377	THE024	33	2.45520453
378	THE003	16	1.52390553
379	THE009	21	2.36434962

380 4.1 Figure 1

381 5 References

- 382 Arnold, A. E., & Lutzoni, F. (2007). Diversity and host range of foliar fungal endophytes: Are
383 tropical leaves biodiversity hotspots? *Ecology*, 88(3), 541–549. [https://doi.org/10.1890/05-](https://doi.org/10.1890/05-1459)
384 [1459](https://doi.org/10.1890/05-1459)
- 385 Arnold, A. E., Mejía, L. C., Kylo, D., Rojas, E. I., Maynard, Z., Robbins, N., & Herre, E.

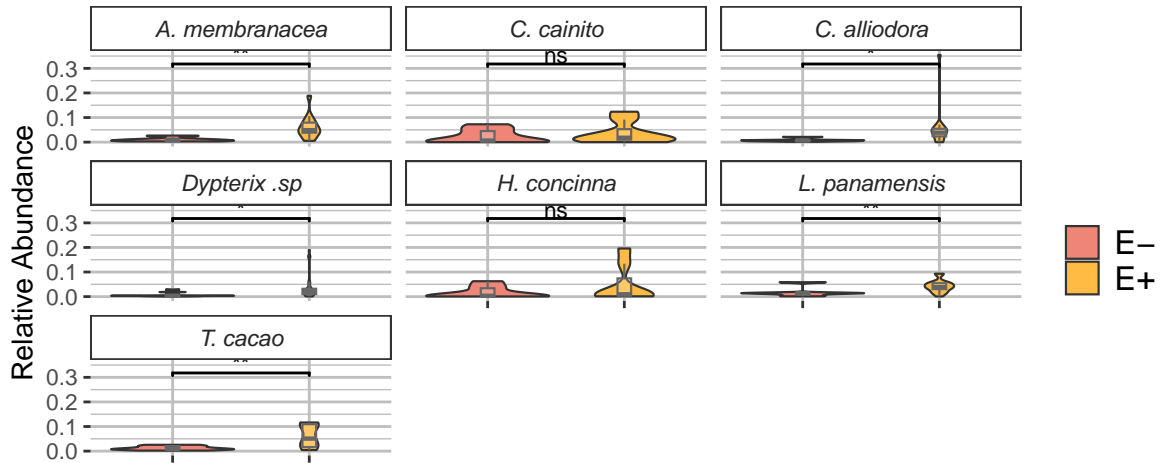


Figure 1: Relative abundance (RA) of Ascomycota OTUs of seven tree species used in the study. Violin plots show the distribution of the RA. The horizontal line within the embedded boxplots represents the median, the box represents the interquartile range (IQR), and the whiskers represent the 1.5xIQR. Outliers are represented by dots. Significant levels are represented by $p=0.05$ (), $p=0.01$ (), and $p=0.001$ ().

- 386 A. (2003). Fungal endophytes limit pathogen damage in a tropical tree. *Proceedings of the*
387 *National Academy of Sciences*, 100(26), 15649–15654.
- 388 Bowman, E. A., & Arnold, A. E. (2021). Drivers and implications of distance decay differ
389 for ectomycorrhizal and foliar endophytic fungi across an anciently fragmented landscape.
390 *The ISME Journal*, 15(12), 3437–3454. <https://doi.org/10.1038/s41396-021-01006-9>
- 391 Callahan, B. J., McMurdie, P. J., Rosen, M. J., Han, A. W., Johnson, A. J. A., & Holmes, S.
392 P. (2016). DADA2: High-resolution sample inference from Illumina amplicon data. *Nature*
393 *Methods*, 13(7), 581–583. <https://doi.org/10.1038/nmeth.3869>
- 394 Carbone, I., White, J. B., Miadlikowska, J., Arnold, A. E., Miller, M. A., Kauff, F., U'Ren,
395 J. M., May, G., & Lutzoni, F. (2017). T-BAS: Tree-Based Alignment Selector toolkit
396 for phylogenetic-based placement, alignment downloads and metadata visualization: An

example with the Pezizomycotina tree of life. *Bioinformatics*, 33(8), 1160–1168. <https://doi.org/10.1093/bioinformatics/btw808>

Carbone, I., White, J. B., Miadlikowska, J., Arnold, A. E., Miller, M. A., Magain, N., U'Ren, J. M., & Lutzoni, F. (2019). T-BAS Version 2.1: Tree-Based Alignment Selector Toolkit for Evolutionary Placement of DNA Sequences and Viewing Alignments and Specimen Metadata on Curated and Custom Trees. *Microbiology Resource Announcements*, 8(29), e00328–19. <https://doi.org/10.1128/MRA.00328-19>

Daru, B. H., Bowman, E. A., Pfister, D. H., & Arnold, A. E. (2019). A novel proof of concept for capturing the diversity of endophytic fungi preserved in herbarium specimens. *Philosophical Transactions of the Royal Society B: Biological Sciences*, 374(1763), 20170395. <https://doi.org/10.1098/rstb.2017.0395>

Higgins, K. L., Arnold, A. E., Coley, P. D., & Kursar, T. A. (2014). Communities of fungal endophytes in tropical forest grasses: Highly diverse host- and habitat generalists characterized by strong spatial structure. *Fungal Ecology*, 8(1), 1–11. <https://doi.org/10.1016/j.funeco.2013.12.005>

McMurdie, P. J., & Holmes, S. (2013). Phyloseq: An R Package for Reproducible Interactive Analysis and Graphics of Microbiome Census Data. *PLoS ONE*, 8(4), e61217. <https://doi.org/10.1371/journal.pone.0061217>

McMurdie, P. J., & Holmes, S. (2014). Waste Not, Want Not: Why Rarefying Microbiome Data Is Inadmissible. *PLoS Computational Biology*, 10(4), e1003531. <https://doi.org/10.1371/journal.pcbi.1003531>

Oita, S., Ibáñez, A., Lutzoni, F., Miadlikowska, J., Geml, J., Lewis, L. A., Hom, E. F. Y.,

419 Carbone, I., U'Ren, J. M., & Arnold, A. E. (2021). Climate and seasonality drive the rich-
 420 ness and composition of tropical fungal endophytes at a landscape scale. *Communications*
 421 *Biology*, 4(1), 313. <https://doi.org/10.1038/s42003-021-01826-7>

422 R Core Team. (2023). *R: A Language and Environment for Statistical Computing* [Computer
 423 software]. R Foundation for Statistical Computing. <https://www.R-project.org/>

424 Rognes, T., Flouri, T., Nichols, B., Quince, C., & Mahé, F. (2016). VSEARCH: A versatile
 425 open source tool for metagenomics. *PeerJ*, 4, e2584. <https://doi.org/10.7717/peerj.2584>

426 Sarmiento, C., Zalamea, P. C., Dalling, J. W., Davis, A. S., Simon, S. M., U'Ren, J. M., &
 427 Arnold, A. E. (2017). Soilborne fungi have host affinity and host-specific effects on seed
 428 germination and survival in a lowland tropical forest. *Proceedings of the National Academy*
 429 *of Sciences of the United States of America*, 114(43), 11458–11463. [https://doi.org/10.107](https://doi.org/10.1073/pnas.1706324114)
 430 [3/pnas.1706324114](https://doi.org/10.1073/pnas.1706324114)

431 Schneider, C. A., Rasband, W. S., & Eliceiri, K. W. (2012). NIH Image to ImageJ: 25 years
 432 of image analysis. *Nature Methods*, 9(7), 671–675. <https://doi.org/10.1038/nmeth.2089>

433 Tellez, P. H., Arnold, A. E., Leo, A. B., Kitajima, K., & Van Bael, S. A. (2022). Traits along the
 434 leaf economics spectrum are associated with communities of foliar endophytic symbionts.
 435 *Frontiers in Microbiology*, 13, 927780. <https://doi.org/10.3389/fmicb.2022.927780>

436 Tellez, P. H., Rojas, E., & Van Bael, S. (2016). Red coloration in young tropical leaves
 437 associated with reduced fungal pathogen damage. *Biotropica*, 48(2), 150–153. [https:](https://doi.org/10.1111/btp.12303)
 438 [//doi.org/10.1111/btp.12303](https://doi.org/10.1111/btp.12303)

439 U'Ren, J. M., & Arnold, A. E. (2017). 96 well DNA Extraction Protocol for Plant and Lichen
 440 Tissue Stored in CTAB. *Protocols.io*, 1–5.

441 U'Ren, J. M., Lutzoni, F., Miadlikowska, J., Zimmerman, N. B., Carbone, I., May, G., &
442 Arnold, A. E. (2019). Host availability drives distributions of fungal endophytes in the
443 imperilled boreal realm. *Nature Ecology & Evolution*, 3(10), 1430–1437. [https://doi.org/](https://doi.org/10.1038/s41559-019-0975-2)
444 [10.1038/s41559-019-0975-2](https://doi.org/10.1038/s41559-019-0975-2)

445 Weiss, S., Xu, Z. Z., Peddada, S., Amir, A., Bittinger, K., Gonzalez, A., Lozupone, C., Zan-
446 eveld, J. R., Vázquez-Baeza, Y., Birmingham, A., Hyde, E. R., & Knight, R. (2017).
447 Normalization and microbial differential abundance strategies depend upon data charac-
448 teristics. *Microbiome*, 5(1), 27. <https://doi.org/10.1186/s40168-017-0237-y>